ppl. Phys. B 63, 437–441 (1996)

Applied Physics B Lasers and Optics

A continuously tunable long-wavelength cw IR source for high-resolution spectroscopy and trace-gas detection

Wade C. Eckhoff[1], Roger S. Putnam[3], Shunxi Wang[2], Robert F. Curl[1], Frank K. Tittel[2]

Department of Chemistry and Rice Quantum Institute, William Marsh Rice University, 6100 Main St., Houston, TX 77251-1892, USA
Department of Electrical and Computer Engineering and Rice Quantum Institute, William Marsh Rice University, 6100 Main St., Houston, TX 77251-1892, USA
Aerodyne Research Inc., 45 Manning Road, Billerica, MA 01821-3976, USA

Received: 1 April 1996 / Accepted: 8 May 1996

Abstract. A new widely tunable source in the infrared for use in high-resolution spectroscopy and trace-gas detection is described. This spectroscopic source is based on Difference Frequency Generation (DFG) in gallium selenide (GaSe) and is continuously tunable in the 7.8–15.0 μm wavelength region. Such a DFG source operates at room temperature which makes it a useful alternative to a lead-salt diode-laser- based detection system that requires cryogenic temperatures and numerous individual diode lasers.

PACS: 7.65; 33.00; 42.60; 42.65; 42.80

There is considerable interest in developing convenient methods for selective and sensitive measurements of trace-gas concentrations. As virtually all fundamental vibrational modes of molecules and molecular ions lie in the 3–20 μm wavelength region, infrared (IR) spectroscopy provides a convenient and real-time method of detection for most gases. Hence, it is important to develop compact and reliable diode-laser-based sources in this spectral region.

Diode-based cw DFG spectroscopic sources have recently been demonstrated in the 3–5 μm region with periodically poled $LiNbO_3$ [1] and $AgGaS_2$ [2]. The present work aims to explore the feasibility of similar cw sources at wavelengths from 5 to 18 μm by mixing two visible lasers in the nonlinear crystal GaSe. Although the work described here uses two cw Ti:Sapphire lasers in order to explore the characteristics of the nonlinear optical material, it is envisioned that the pump lasers will ultimately be high-power visible/near-IR diode lasers to create a rugged portable IR source for gas monitoring.

Gallium selenide has been tested previously in pulsed DFG sources in the 4–19 μm region [3–8]. In addition, Vodopyanov et al. [9, 10] have measured the spontaneous parametric emission from GaSe pumped by a mode-locked Er:YAG (2.94 μm) laser. In all these experiments pulsed lasers operating at wavelengths longer than 1 μm were used to generate the tunable IR radiation. In the only previous reported work with visible pumps, Abdullaev and co-workers used the pulsed output of a ruby laser and dye laser (715–750 nm) in a DFG source to generate pulsed radiation in the 9–18 μm region [11].

A good summary of the above experiments and many others can be found in the review article by Fernelius [12].

1 Experimental

The cw IR spectroscopic source, shown in Fig. 1, used the 20 W all-lines output of an argon ion laser to pump simultaneously two single-frequency cw Titanium:Sapphire ring lasers (Coherent Model 899-21 and 899-29). These lasers are actively frequency stabilized by locking to external etalons, and line widths in the near IR of 1 MHz are typical. Titanium:Sapphire lasers were used in this experiment because of their superior wavelength tuning, transverse-mode quality, and output power characteristics. The output from each laser was attenuated to < 300 mW using linearly variable filters to avoid optical damage of the GaSe crystal. The two beams were spatially overlapped by rotating the polarization of the pump beam orthogonal to the signal and combining them in a polarization cube to provide Type-I phase matching. Type-I phase matching was chosen in GaSe because the required external angle and walkoff effects are smaller than for Type II. The two beams are chopped and focussed with a 100 mm lens into a GaSe crystal 5 mm in length and 10 mm in diameter mounted on a rotation stage. The IR light generated in the GaSe crystal was collected and refocused with a single ZnSe lens onto a 1-mm-diameter liquid-nitrogen-cooled HgCdTe detector. A broadband antireflective-coated (3–13 μm) Ge flat is placed immediately in front of the detector to block the two pump beams. The output of the detector is monitored by a lock-in amplifier and recorded by a computer. A 50-cm-long absorption cell equipped with ZnSe windows was used for absorption experiments.

Dedicated to Prof. F. P. Schäfer on the occasion of his 65th birthday.

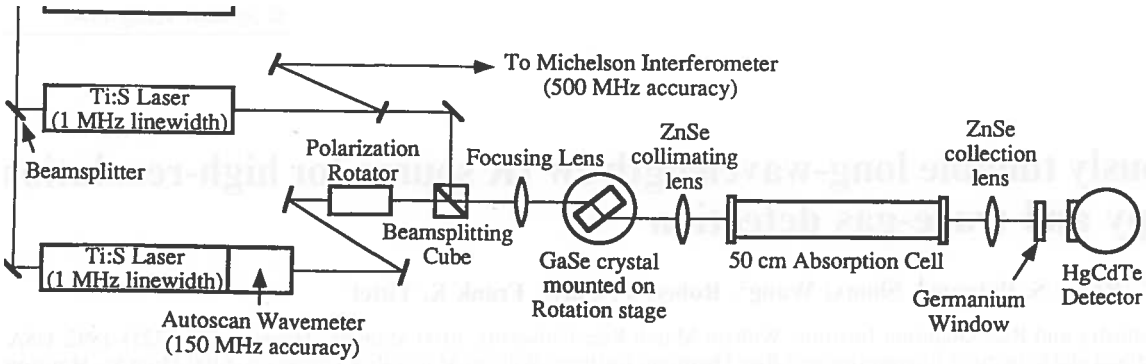

Fig. 1. Schematic diagram of a DFG spectroscopic source based on GaSe crystal.

To date, we have generated continuously tunable light from 8.8 to 15.0 μm by tuning the wavelength of the two pump lasers and the angle of the crystal. We are not fundamentally limited to this tuning range and could extend the range to 6 μm with larger crystal angles, but the present crystal mount restricts the GaSe external angle to less than 60°. We expected to be able to tune to the 18 μm absorption edge of the crystal but did not obtain significant IR power at wavelengths longer than 15 μm. Within the current 45–60° range of external angles it is possible to tune continuously over a 6.2 μm IR range using only a 25 nm tuning range of one of the visible/near-IR pump lasers.

The published Sellmeier coefficients [13–17] were found to be inadequate for accurately describing the combination of input wavelengths and crystal angles to generate IR light. The predicted pump wavelengths for a given external crystal angle and signal wavelength are too low by about 3% or 20–25 nm, which confirms the observations of the Abdullaev [16] and Bhar [18] groups. Abdullaev attributed these errors to insufficiently accurate determination of the ordinary index of refraction near the short-wavelength edge of the absorption band. The results of our systematic investigation for optimized phase-matched conditions are given in Fig. 2. We obtained each data point by fixing the crystal angle and the signal wavelength and by scanning the pump-laser wavelength. The results of one such scan is shown in Fig. 3. The noise in the trace is a result of limiting the input power of each beam to 25 mW average at the crystal to avoid possible thermal effects due to absorption. The phase-matching FWHM was found to be 0.706 nm (10.967 cm^{-1}) for a pump laser scan with the signal-laser wavelength fixed at 868.318 nm and the external crystal angle fixed at 51.2°.

We attempted to reoptimize the Sellmeier coefficients and found that the mathematical system was underdetermined. There were numerous solutions that fit our experimental data and some of these deviated from the previously published index-of-refraction dispersion relations. We, therefore, have chosen to present our data on predicting the GaSe-crystal external angle in a manner that makes no reference to the index of refraction so that no confusion results. The external crystal angle in degrees was fitted with a quadratic function of the pump

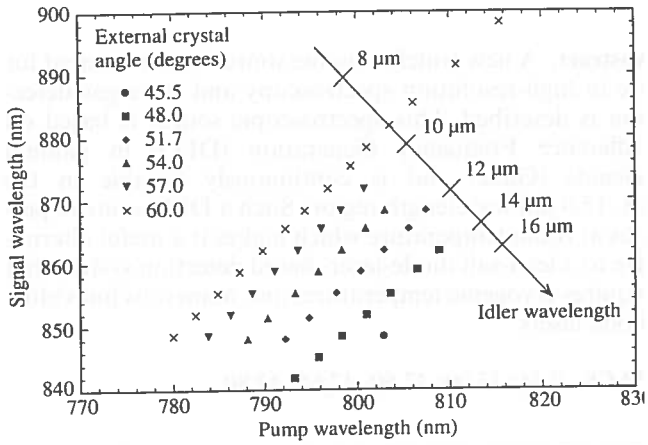

Fig. 2. Experimental phase-matching angles and wavelengths fo a GaSe crystal in the 780–880 nm pumping region. Individual point represent combinations of external angles and pump wavelength that optimize the IR DFG power. IR wavelengths are given b projecting the data points onto the diagonal axis labeled "idle wavelength"

wavelength (λ_p) in nanometers and the idler frequency (ν_i in wave numbers:

$$\text{External angle} = 49.4 - 1.84\times10^{-5}\times\lambda_p^2 + 4.70\times10^{-5} \times\nu_i^2 - 4.37\times10^{-11}\times\lambda_p^2\times\nu_i^2.$$

The fit to our 44 data points has a standard deviation o 0.12°. There is a high relative uncertainty in all the coeffi cients due to a linear dependence between variables whicl is not easily removed without transforming the observec variables of wavelength and frequency to non-intuitiv units. The main source of experimental uncertainty wa the measurement of the zero crystal angle. We were able t measure the back reflection at the polarization cube fron normal incidence with respect to the GaSe crystal t within two millimeters which yielded an angular resolu tion of 0.2°. The uncertainty in the pump and signa wavelengths are several orders of magnitude below thi angular uncertainty.

Under the plane-wave approximation, the phase matching bandwidth is a simple function of the effectiv

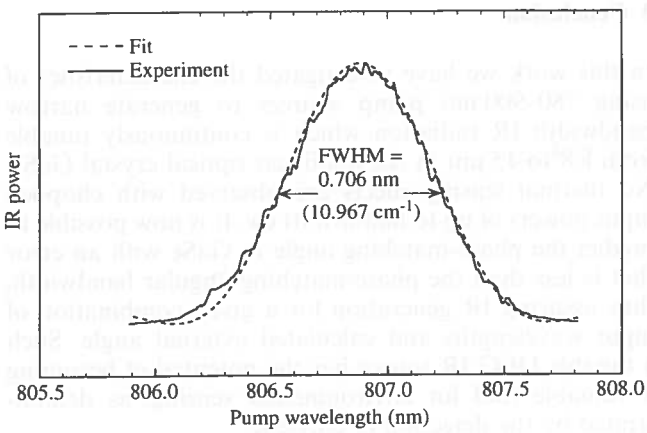

Fig. 3. Wavelength dependence of the IR power with fixed signal laser wavelength of 868.318 nm and fixed GaSe-crystal external angle of 51.2°

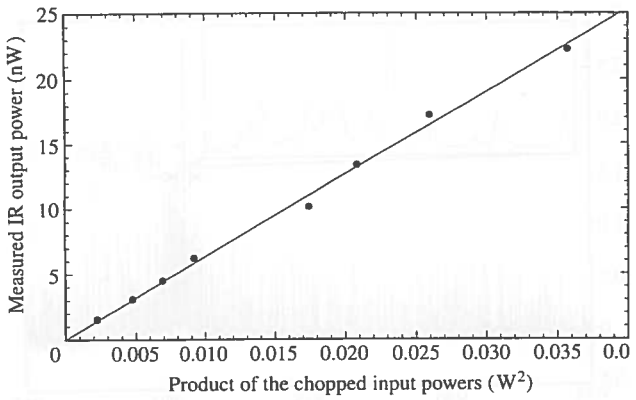

Fig. 4. IR DFG power vs the product of two input pump powe The line is a least-squares fit to the data. The idler, pump, and sig wavelengths were 13.708 μm, 793.210 nm, and 841.925 nm, resp tively, and the external angle was 48.3°

coherence length and the wave-vector mismatch. The output power can be regarded as proportional to $\mathrm{sinc}^2(\Delta k L_{\mathrm{eff}}/2)$. Assuming all three indices of refraction to be constant during a scan and $\Delta k = 0$ at the peak of the IR production, the Δk term can be approximated by (1):

$$\Delta k = 2\pi \times \left(\frac{1}{\lambda_p} - \frac{1}{\lambda_p^0}\right) \times (n_p - n_i), \tag{1}$$

where λ_p is the pump wavelength, λ_p^0 is the pump wavelength at which the output IR power is maximized, and n_p and n_i are the indices of refraction at the pump and idler wavelengths, respectively. In this fashion, only the difference between the indices of refraction are necessary to compute the wave-vector mismatch and is relatively insensitive to the choice of Sellmeier constants. The wave-vector mismatch is assumed to be equal to zero at the centroid of the experimental curve based on the observation that the curve does not exhibit the asymmetry shown in systems where the maximum output power and $\Delta k = 0$ do not coincide (see [19] for an example in the case of second-harmonic generation). The phase-matching bandwidth for unfocused and focused beams is found to be nearly identical so long as the beams are not in the overfocused condition. In this experiment, we deliberately underfocused the input beams by using an $f = 100$ mm lens instead of the $f = 66$ mm called for by theory. By fitting the observed spectrum with (1) where L_{eff} is the adjustable variable, it is possible to obtain agreement between theory and experiment. The value of L_{eff} determined from this fit is 2.9 mm – in agreement with [3] in which an L_{eff} value of 3.2 mm was obtained.

As a further test of our fitting, the L_{eff} parameter can be estimated by

$$L_{\mathrm{eff}} = \left(\frac{\lambda_p}{2\Delta n}\right),$$

where Δn is the change in index of the pump beam in turning the crystal to reduce the IR power to 40.5% of the peak value or when the accumulated phase error is equal to 180°. The value of Δn is calculated from the dispersion relations, and again it is found to be largely invariant with choice of Sellmeier coefficients. The resulting L_{eff} 2.9 mm. Both our results imply that in this instance t coherence length is determining the power output and n the crystal length.

The effect of high input powers on the paramet conversion process was measured. Linearly variable ne tral density filters were used to vary the input powers a the generated IR power plotted vs their product in Fig. Thermal lensing can be a problem in the nonlinear optic conversion process – especially in the case of intense input beams [20]. This effect can cause the IR power scale less than linearly with the product of the inp powers but was not observed in GaSe as shown in Fig. The experimental conversion efficiency derived fr the slope of the fitted line in the figure is 28% of t calculated value obtained with a nonlinear coefficie $d_{22} = 54.4$ pm/V[16] at the specific wavelengths used Fig. 4. The calculated power in the above comparison w corrected for Fresnel losses at all uncoated surfaces. O best estimate of the detector calibration is ± 20 A component of the discrepancy is the transverse dist tion of the beam into an oval shape with non-norm incidence upon the GaSe crystal surface. This could corrected with the use of a cylindrical focusing lens. A s ond explanation of the missing power is the possibil that the two input beams were focused at different longit dinal positions. We assumed that the lasers were oper ing to manufacturers' specifications and thus the foci we in the same location, but telescopes could be inserted the beam path to verify this condition.

2 Spectroscopy of ethylene (C_2H_4)

The maximum mid-IR output measured by the prese system is about 30 nW, which is sufficient for spectr scopic detection of many gases. It is feasible to desi a mid-IR absorption-based gas sensor based on the m ing of two visible high-power laser diodes (in mas oscillator-power amplifier geometries at the 0.5–1 W lev

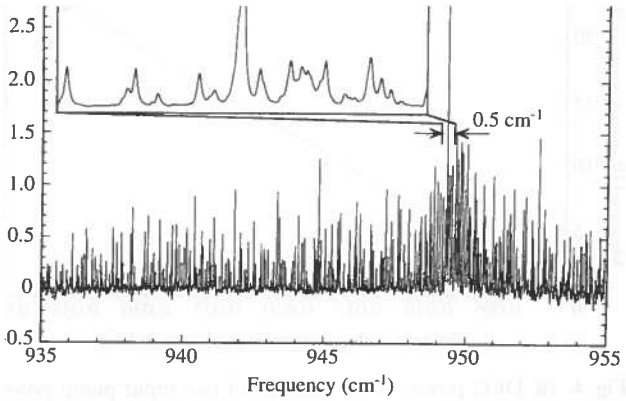

g. 5. A sample spectrum of the ethylene molecule near 945 cm^{-1} :en with a path length of 50 cm and a pressure of 20 mTorr. The et is a 0.5 cm^{-1} blowup centered on the strongest absorption lines the lower scan

GaSe. This sensor would be capable of detecting nu-erous gases of interest in atmospheric monitoring – in-ıding but not limited to such species as hydrogen cyan-e, acetylene, ethylene, ammonia, nitric acid, phosphine, one, methane, and nitrous oxide.

Ethylene is a very interesting biological molecule. It s been found to play a role in many developmental ocesses in plants: ripening of fruits, wilting of flowers, d the emergence from dormancy in some seeds and lbs [21–23]. Environmental stresses, such as excessive ıter loss, mechanical damage, and lack of sufficient light, stimulate the production of increased levels of C_2H_4 4]. Ethylene concentrations have been monitored by s chromatography and by photoacoustic detection us-g a carbon dioxide laser [25–27], though neither ethod is readily portable. Using difference frequency neration, it appears feasible to construct an ethylene ısor that is compact and battery driven.

In the 10-μm region, the absorption of ethylene gas is sentially due to the intense ν_7 C-type perpendicular IR nd which presents a strong Q-branch near 950 cm^{-1}. ıe P and R branches cover the region from 800 to 00 cm^{-1}. Much in the way of high-resolution spectro-ɔpy has been conducted on this band [28–31]. Nearly the lines in this region have been assigned and their sitions known to sub-Doppler accuracy.

A 20 cm^{-1} scan of ethylene taken with the experi-ntal apparatus is shown in Fig. 5. The inset spectrum is ɔlowup of 0.5 cm^{-1} centered around the most intense sorption lines. The total path length is 50 cm and the ıylene pressure is 20 mTorr. The scan was taken by ing the signal laser at 868.750 nm, the external angle to .5°, and scanning the pump laser from 802.195 to 3.484 nm in 20 MHz steps. The lock-in amplifier was set a 100 ms time constant with a 12 dB/octave rolloff. cause of etalon effects within the 3-mm-thick ZnSe flats ed as windows for the absorption cell, the cell was mped out and scanned to provide normalization.

In this work we have investigated the characteristics of using 780–900 nm pump sources to generate narrow bandwidth IR radiation which is continuously tunable from 8.8 to 15 μm in the nonlinear optical crystal GaSe. No thermal lensing effects are observed with chopped input powers of up to half-a-watt cw. It is now possible to predict the phase-matching angle in GaSe with an error that is less than the phase-matching angular bandwidth, thus assuring IR generation for a given combination of input wavelengths and calculated external angle. Such a tunable DFG IR source has the potential of becoming a valuable tool for environmental sensing, as demonstrated by the detection of ethylene.

Acknowledgements. The authors would like to thank K. Kato and D. Roberts for helpful discussions. This work was supported in part by the National Science Foundation and the Robert A. Welch Foundation. WCE is grateful to the Department of Defense for support in the form of an NDSEG fellowship. RSP and SW are grateful for support from the Department of Energy, Contract #DE-FG02-94ER81698, through Aerodyne Research.

References

1. K.P. Petrov, L. Goldberg, W.K. Burns, R.F. Curl, F.K. Tittel: Opt. Lett. **21**, 86 (1996)
2. K.P. Petrov, S. Waltman, U. Simon, R.F. Curl, F.K. Tittel, E.J. Dlugokensky, L. Hollberg: J. Appl. Phys. B **61**, 553 (1995)
3. A. Bianchi, A. Ferrario, M. Musci: Opt. Commun. **25**, 256 (1978)
4. A. Bianchi, M. Garbi: Opt. Commun. **30**, 122 (1979)
5. T. Dahinten, U. Plodereder, A. Seilmeier, K.L. Vodopyanov, K.R. Allakhverdiev, Z.A. Ibragimov: IEEE J. Quant. Electron. **29**, 2245 (1993)
6. J.L. Oudar, Ph. J. Kupecek, D.S. Chemla: Opt. Commun. **29**, 119 (1979)
7. Yu.A. Gusev, A.V. Kirpichnikov, S.N. Konoplin, S.I. Marennikov, P.V. Nikles, Yu.N. Polivanov, A.M. Prokhorov, A.D. Savel'ev, R. Sh. Sayakhov, V.V. Smirnov, V.P. Chebotaev: Sov. Tech. Phys. Lett. **6**, 541 (1980)
8. A. Suda, H. Tashiro: Digest of 16th Ann. Meeting Laser Soc. Japan, 53 (1996)
9. K.L. Vodopyanov, L.A. Kulevskii, V.G. Voevodin, A.I. Gribenyukov, K.R. Allakhverdiev, T.A. Kerimov: Opt. Commun. **83**, 322 (1991)
10. K.L. Vodopyanov: J. Opt. Soc. Am. B **10**, 1723 (1993)
11. G.B. Abdullaev, L.A. Kulevskii, P.V. Nikles, A.M. Prokhorov, A.D. Savel'ev, E.Yu. Salaev, V.V. Smirnov: Sov J. Quant. Electron. **6**, 88 (1976)
12. N.C. Fernelius: Prog. Crystal Growth and Charact. **28**, 275 (1994)
13. S. Adachi, Y. Shindo: J. Appl. Phys. **71**, 428 (1992)
14. G.B. Abdullaev, L.A. Kulevskii, A.M. Prokhorov, A.D. Savel'ev, E.Yu. Salaev, V.V. Smirnov: JETP Lett. **16**, 90 (1972)
15. N. Piccioli, R. Le Toullec, M. Mejatty, M. Balkanski: Appl. Opt. **16**, 1236 (1977)
16. G.B. Abdullaev, K.R. Allakhverdiev, L.A. Kulevskii, A.M. Prokhorov, E.Yu. Salaev, A.D. Savel'ev, V.V. Smirnov: Sov. J. Quant. Electron. **5**, 665 (1975)
17. K.L. Vodopyanov, L.A. Kulevskii: Opt. Commun. **118**, 375 (1995)
18. G.C. Bahr, S. Das, K.L. Vodopyanov: J. Appl. Phys. B **61**, 187 (1995)
19. G.D. Boyd, D.A. Kleinman: Appl. Phys. **39**, 3597 (1968)
20. C.E. Miller, W.C. Eckhoff, U. Simon, F.K. Tittel, R.F. Curl: SPIE **2145**, 282 (1994)

21. S.F. Yang, N.E. Hoffmann: Ann. Rev. Plant Physiol. **35**, 155 (1984)
22. F.B. Abeles: *Ethylene in Plant Biology* (Academic, London 1973) p. 302.
23. M.B. Jackson: In *Ethylene and Plant Development*, ed. by J.A. Roberts, G.A. Tucker (Butterworths, London 1985).
24. H. Mehlhorn, A.R. Wellburn: Nature **327**, 417 (1987)
25. L.B. Kreuzer, N.D. Kenyon, C.K.N. Patel: Science **177**, 347 (1972)
26. D. Bicanic, F. Harren, J. Reuss, E. Woltering, J. Snel, L.A.C.J. Voesenek, B. Zuidberg, H. Jalink, F. Bijnen, C.W.P.M. Blom, H. Sauren, M. Kooijman, L. van Hove, W. Tonk: In *Photoacoustic, Photothermal and Photochemical Processes in Gases*, ed. P. Hess (Springer, New York 1989).
27. C. Brand, A. Winkler, P. Hess, A. Miklos, Z. Bozoki, J. Sneid Appl. Opt. **34**, 3257 (1995)
28. W.L. Smith, I.M. Mills: J. Chem. Phys. **40**, 2095 (1964)
29. Ch. Lambeau, A. Fayt, J.L. Duncan, T. Nakagawa: J. M Spectrosc. **81**, 227 (1980)
30. F. Herlemont, M. Lyszyk, J. Lemaire, Ch. Lambeau, A. Fayt: Mol. Spectrosc. **74**, 400 (1979)
31. I. Cauuet, J. Walrand, G. Blanquet, A. Valentin, L. Henry, C Lambeau, M. de Vleeschouwer, A. Fayt: J. Mol. Spectrosc. **1** 191 (1990)